Chinese Journal of Aeronautics, (2014),27(1): 124–135

Chinese Society of Aeronautics and Astronautics
& Beihang University

Chinese Journal of Aeronautics

cja@buaa.edu.cn
www.sciencedirect.com

Collision risk-capacity tradeoff analysis of an en-route corridor model

Ye Bojia [a,b], **Hu Minghua** [a,b,*], **John Friedrich Shortle** [c]

[a] *College of Civil Aviation, Nanjing University of Aeronautics and Astronautics, Nanjing 211100, China*
[b] *National Key Laboratory of Air Traffic Flow Management, Nanjing University of Aeronautics and Astronautics, Nanjing 211100, China*
[c] *Center for Air Transportation Systems Research, George Mason University, Fairfax 22030, USA*

Received 25 April 2013; revised 24 July 2013; accepted 16 September 2013
Available online 18 December 2013

KEYWORDS

Air traffic control;
Corridor;
Risk-capacity tradeoff;
Self-separation;
Simulation

Abstract Flow corridors are a new class of trajectory-based airspace which derives from the next generation air transportation system concept of operations. Reducing the airspace complexity and increasing the capacity are the main purposes of the en-route corridor. This paper analyzes the collision risk-capacity tradeoff using a combined discrete–continuous simulation method. A basic two-dimensional en-route flow corridor with performance rules is designed as the operational environment. A second-order system is established by combining the point mass model and the proportional derivative controller together to simulate the self-separation operations of the aircrafts in the corridor and the operation performance parameters from the User Manual for the Base of Aircraft Data are used in this research in order to improve the reliability. Simulation results indicate that the aircrafts can self-separate from each other efficiently by adjusting their velocities, and rationally setting the values of some variables can improve the rate and stability of the corridor with low risks of loss of separation.

1. Introduction

A corridor is defined as a long "tube" of airspace, in which groups of flights fly along the same path in one direction and accept responsibility for separation from each other. Multiple (parallel) lanes, self-separation, and dynamic activation rules are three of the prominent attributes of corridors. A well-designed corridor may reduce the airspace complexity, increase the airspace capacity, and decrease the workload of air traffic controllers.[1]

Previous research has looked at the initial design concept, optimal placement of corridors, and the topology of the network. John et al.[2] initially proposed and evaluated the conception of dynamic airspace super sectors (DASS), which is thought of as a network of one-directional, high-density highways in the sky. Safety, performance, and cost are three primary criteria used to measure design alternatives. Yousefi et al.[3] conducted a statistical analysis of city-pair traffic and

* Corresponding author at: College of Civil Aviation, Nanjing University of Aeronautics and Astronautics, Nanjing 211100, China. Tel.: +86 25 52112079.
E-mail addresses: yebojia2010@gmail.com (B. Ye), minghuahu@nuaa.edu.cn (M. Hu), JShortle@gmu.edu (J.F. Shortle).

Peer review under responsibility of Editorial Committee of CJA.

ELSEVIER Production and hosting by Elsevier

1000-9361 © 2014 Production and hosting by Elsevier Ltd. on behalf of CSAA & BUAA. Open access under CC BY-NC-ND license.
http://dx.doi.org/10.1016/j.cja.2013.12.007

the placement of a network of high-volume tube-shape sectors (HTS). Velocity vectors for small volumes of airspace were calculated and vector fields of the fluid velocity were created. After the analysis of the vector fields' topology, the geometries and locations of potential corridors were determined. Sridhar et al.[4] grouped airports into regions, and modeled a series of tubes connecting major regions. A network connecting the top 18 regions was designed, and the top 250 busy airports with the appropriate regions were associated by clustering techniques. Hoffman et al.[5] constructed a tube network and made an estimate of capacity-enhancing effects of tubes for airspace. A comprehensive list of design issues and some potential alternatives were created to enhance the tube design and tradeoffs. Xue et al.[6,7] studied the complexity of traffic in a selected corridor using simulation. A space–time map was developed to examine and visualize the utilization of corridors, suggest the number of lanes, and show the possibility of deploying corridors dynamically. Yousefi et al.[8,9] developed an initial operational procedure to implement flow corridor operations, and proposed a flow-based modeling approach to cluster 4DTs into potential corridors. A sliding time window was implemented to dynamically create and optimize a corridor's coordinates based on the changes in preferred trajectories.

The objective of this research is to develop models and methods for constructing collision risk-capacity tradeoff curves in a corridor.

2. Model description

2.1. Structure and assumptions of corridor

A two-dimensional en-route flow corridor is presented to be a tube of parallel high-altitude Q-routes structure which is assumed to be 80 nm (nautical mile) long and 16 nm wide with the route centerlines 8 nm apart and located at the FL350 as shown in Fig. 1.

Aircraft usually travel in the same direction from left to right by self-separation in the corridor. An aircraft may adjust its velocity and separation with the leading one, switch lanes for overtaking, or in extreme cases exit the corridor along paths that are at a divergence angle by 30° before the exit. Detailed movements of each aircraft are assumed as follows:

(1) All aircraft initially enter the corridor with random types, velocities, and separations with their leading ones.
(2) Each aircraft is under conditions of level fight that flies along the middle line of each corridor and self-separates with the aircraft in front according to a self-separation model by adjusting its acceleration and velocity.
(3) Any time the velocity of an aircraft is higher than the average velocity of the leading one by a velocity threshold, it attempts to switch the lane.
(4) Any time an aircraft gets within the minimum separation of the aircraft in front (loss of separation), it switches its lane or breaks out.

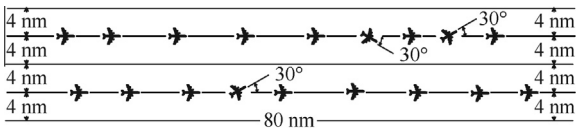

Fig. 1 Structure of corridor.

(5) The first aircraft in each lane and the aircraft whose separation with its leading aircraft is larger than a threshold value, it flies towards the target velocity.

2.2. Aircraft performance model

2.2.1. Aircraft model

In this paper, the aircraft is modeled by using the point mass model (PMM). This model is adapted from the work of Glover and Lygeros.[10] Some key elements of the model are summarized here. The states of the model are the horizontal position x and y and the altitude z of the aircraft, the true airspeed v, the flight path angel γ, and the heading ψ. Table 1 illustrates the descriptions and primary dimensions of the state variables.

The control inputs to the model are the engine thrust T, the angle of attack ϕ, and the bank angle α. Table 2 outlines the descriptions and primary dimensions of the control variables.

The Newtonian dynamics equations of motion used in this paper are:

$$\begin{cases} \dot{x} = v\cos\psi\cos\gamma \\ \dot{v} = \dfrac{1}{m}(T\cos\alpha - D - mg\sin\gamma) \\ \dot{\psi} = \dfrac{1}{mv}(L + T\sin\alpha)\sin\phi \\ \dot{\gamma} = \dfrac{1}{mv}[(L + T\sin\alpha)\cos\phi - mg\cos\gamma] \end{cases} \tag{1}$$

where m is the mass of the aircraft and g is the gravitational acceleration. L and D denote respectively the lift and drag forces, which are functions of the state and the angle of attack as outlined as follows:

$$\begin{cases} L = \dfrac{C_L S\rho}{2}(1 + c\alpha)v^2 \\ D = \dfrac{C_D S\rho}{2}(1 + b_1\alpha + b_2\alpha^2)v^2 \end{cases} \tag{2}$$

where S is the surface area of the wings, ρ is the air density, and C_D, C_L, c, b_1, and b_2 are aerodynamic lift and drag coefficients whose values generally depend on the phase of the fight. During the cruising phase, all commercial airliners are usually assumed operating near trimmed flight conditions ($\gamma = \dot{\gamma} = 0$ and $\alpha \approx 0$), and then the lift is represented by:

Table 1 State variables.

Variables	Description	Primary dimension
x	Along-track position	Along-track
v	True airspeed	Along-track
y	Across-track position	Across-track
ψ	Heading	Across-track
z	Altitude	Vertical
γ	Flight-path angle	Vertical

Table 2 Control variables.

Variables	Description	Primary dimension
T	Thrust	Along-track
ϕ	Bank angle	Across-track
α	Angle of attack	Vertical

$$\dot{\gamma} = \frac{1}{mv}[(L + T\sin\alpha)\cos\phi - mg\cos\gamma] = 0$$

$$\Rightarrow L = mg\frac{\cos\gamma}{\cos\phi} - T\sin\alpha = \frac{mg}{\cos\phi} \tag{3}$$

Assume that the coefficient of lift C_L is set so that the lift exactly balances the weight of the aircraft. Combining the previous relationships, C_L can be calculated by:

$$L = \frac{mg}{\cos\phi} = \frac{C_L S\rho}{2}(1 + c\alpha)v^2$$

$$\Rightarrow C_L = \frac{2mg}{S\rho v^2\cos\phi} \tag{4}$$

The drag coefficient is computed as a function of the phase of flight as follows:

$$C_D = \begin{cases} C_{D_0,\mathrm{AP}} + C_{D_2,\mathrm{AP}}C_L^2 & \text{Approach} \\ C_{D_0,\mathrm{LDG}} + C_{D_0,\Delta\mathrm{LDG}} + C_{D_2,\mathrm{AP}}C_L^2 & \text{Landing} \\ C_{D_0,\mathrm{CR}} + C_{D_2,\mathrm{CR}}C_L^2 & \text{Other} \end{cases} \tag{5}$$

where $C_{D_0,\mathrm{CR}}$ and $C_{D_2,\mathrm{CR}}$ are two constants relative to the cruising phase, and the others are relative to approach or landing phases.

This further implies the lift and drag functions as:

$$\begin{cases} L = \dfrac{C_L S\rho}{2}(1+c\alpha)v^2 = \dfrac{2mg}{S\rho v^2\cos\phi}\dfrac{S\rho}{2}(1+c\alpha)v^2 = \dfrac{mg}{\cos\phi} \\ D = \dfrac{C_D S\rho}{2}\left(1 + b_1 a + b_2\alpha^2\right)v^2 = \dfrac{C_D S\rho}{2}v^2 \end{cases} \tag{6}$$

2.2.2. Discrete states

Discrete states are used for describing the self-separation performance of the aircraft in the corridor. Five different discrete states are defined in the corridor: velocity adjusting (VA) state, target velocity flying (TVF) state, lane changing state (LCS), breakout state (BS), and locking state (LS). Different from the other four types of states, LS is a combined state which cannot exist without TVF and VA. Fig. 2 illustrates the state transition diagram of the aircraft, in which TVF, VA, LCS, and BS are all represented by solid circles while LS is represented by a dashed circle outside TVF and VA.

(1) Velocity adjusting (VA) state.

VA state is a state in which the aircraft attempts to adjust its velocity, acceleration, and separation with the leading aircraft according to the proportional derivative (PD) controller below. The aircraft is in this state if the separation with the leading one is less than the distance threshold (that is, the leading aircraft is not too far in front) but larger than the minimum separation. This state can transfer from/to the target velocity flying state and the lane changing state, locked or unlocked, or transfer to the breakout state (be aware that this is a unidirectional transition). For the point mass model, combine the equations of time derivatives of along-track positions and velocities to obtain

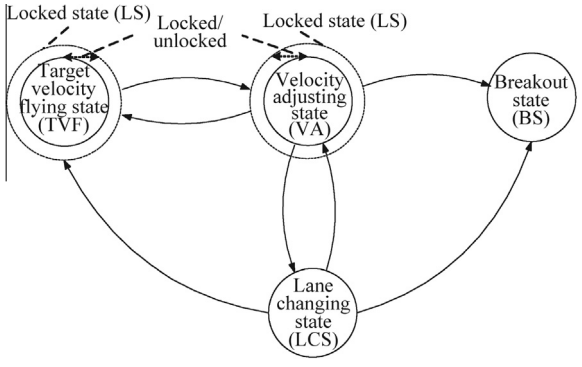

Fig. 2 State transition diagram.

$$\begin{cases} \dot{x} = v\cos\psi\cos\gamma \\ \dot{v} = \dfrac{1}{m}(T\cos\alpha - D - mg\sin\gamma) \end{cases}$$

Because all the aircraft are assumed straight ($\psi = 0$ or small) and level flight ($\gamma = \dot{\gamma} = 0$, $\alpha = 0$) in the corridor, substitute the drag into the above equations and get

$$\begin{cases} \dot{x} \approx v \\ \dot{v} = \dfrac{1}{m}T - \dfrac{C_D S\rho}{2m}v^2 \end{cases}$$

This is equivalent to a second-order equation:

$$\ddot{x} = \frac{T}{m} - \frac{C_D S\rho}{2m}v^2 = \frac{T}{m} - \frac{C_D S\rho}{2m}\dot{x}^2$$

Using a proportional plus derivative control yields

$$T = k_1(x_{\mathrm{ref}} - x) + k_2(v_{\mathrm{ref}} - v) + T_{\mathrm{ref}}$$

where T_{ref} is the thrust of the aircraft to balance the drag, x_{ref} is the target position along the track, v_{ref} is the target velocity, and k_1 and k_2 are tuning parameters. This leads to the second-order system[11] as:

$$\ddot{x} = \frac{k_1(x_{\mathrm{ref}} - x) + k_2(v_{\mathrm{ref}} - v)}{m} + \frac{C_D S\rho}{2m}v^2 - \frac{C_D S\rho}{2m}v^2$$

$$\Rightarrow m\ddot{x} + k_2\dot{x} + k_1 x = k_1 x_{\mathrm{ref}} + k_2 v_{\mathrm{ref}} \tag{7}$$

Un-damped natural frequency:

$$\omega_n = \sqrt{\frac{k_1}{m}}$$

Damping ratio:

$$\zeta = \frac{k_2}{2\sqrt{mk_1}}$$

To achieve a time constant of τ:

$$\tau = \frac{1}{\zeta\omega_n} = \frac{2\sqrt{mk_1}}{k_2}\frac{\sqrt{m}}{\sqrt{k_1}} = \frac{2m}{k_2}$$

$$\Rightarrow k_2 = \frac{2m}{\tau}$$

To achieve a damping ratio of ζ:

$$\sqrt{mk_1} = \frac{k_2}{2\zeta}$$

$$\Rightarrow k_1 = \frac{k_2^2}{4m\zeta^2}$$

Using τ and ζ as inputs, the acceleration of the aircraft can be calculated as:

$$\ddot{x} = \frac{k_1(x_{\mathrm{ref}} - x) + k_2(v_{\mathrm{ref}} - v)}{m} \tag{8}$$

(2) Target velocity flying (TVF) state.

TAF state is a state in which an aircraft attempts to fly at its preferred target velocity without regard to the position or velocity of the aircraft in front of it. The aircraft is in this state if either (a) it is the first aircraft in the corridor, or (b) its

leading aircraft is sufficiently far ahead so that it does not currently need to adjust its velocity to maintain separation. This state can transfer from/to the velocity adjusting state, locked or unlocked, or transfer from the lane changing state (unidirectional transition).

Different from the VA state, using a derivative control:

$$T = k_2(v_{\text{ref}} - v) + T_{\text{ref}}$$

This leads to the following first-order system:

$$\ddot{x} = \frac{k_2(v_{\text{ref}} - v)}{m} + \frac{C_D S\rho}{2m}v^2 - \frac{C_D S\rho}{2m}v^2$$

$$m\ddot{x} + k_2\dot{x} = k_2 v_{\text{ref}} \Rightarrow m\dot{v} + k_2 v = k_2 v_{\text{ref}} \tag{9}$$

The acceleration of the aircraft can be calculated as:

$$\dot{v} = \frac{k_2(v_{\text{ref}} - v)}{m} \tag{10}$$

(3) Lane changing state (LCS).

Before introducing the LCS, the lane switch requirement should be defined first. Lane switch requirement is a criterion to decide whether an aircraft can switch its lane for overtaking or avoiding conflicts. Some research has been done on constructing resolution trajectories and relative rules in a single lane,[12,13] and the detailed contents of lane changing criterion in the corridor will be developed here: (a) the potential lane-switch aircraft should be in either the VA state or the TVF state but not locked; (b) the potential lane-switch aircraft should make a projection of the target flight onto another lane (assuming a 30° path) to find its new leading and trailing aircraft in that lane, and both of the distances between the potential lane-switch aircraft and the new leading and trailing aircraft must be larger than the lane-switch separation; (c) the trailing aircraft in the new corridor should also be in the VA state or the TVF state.

LCS is a state in which a target aircraft flies a 30°(θ) path to another lane with a constant velocity as shown in Fig. 3. The aircraft switches lanes under the following two situations: (a) its separation with its leading aircraft is less than the minimum separation and also the lane switch requirement is satisfied; (b) its velocity is larger than the average velocity of its leading aircraft by the velocity threshold, its separation with its leading aircraft is less than the distance threshold, and also the lane switch requirement is satisfied. This state can transfer from/to the velocity adjusting state, and transfer to the target velocity flying state or the breakout state (unidirectional transition).

When the aircraft starts to change its lane, the fly-pass method is adopted to simulate the turning procedure. The aircraft starts turning before it reaches the point and "cuts the corner", this is the preferred method for most modern aircraft.

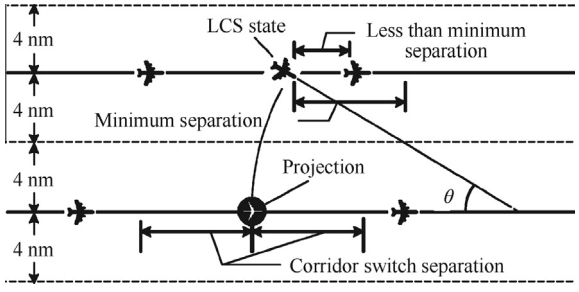

Fig. 3 Lane changing state.

To determine how long it takes an aircraft to switch its lane, the radius r and the distance d should be calculated first, as in Fig. 4.

Assume the aircraft remains level throughout the LCS and turns are executed at a fixed bank angle $\pm\phi_{\text{nom}}$, so the component of the lift in the vertical direction is equated to the weight of the aircraft, and the turn rate can be calculated as:

$$\dot{\psi} = \frac{1}{mv}(L + T\sin\alpha)\sin\phi = \frac{1}{mv}\left(\frac{mg}{\cos\phi_{\text{nom}}}\right)\sin\phi_{\text{nom}} = \frac{g\tan\phi_{\text{nom}}}{v} \tag{11}$$

Assuming that the aircraft starts the turn at time 0 with heading ψ_0, at time t the heading angle $\psi(t)$ and the distance traveled by the aircraft are:

$$\begin{cases} \psi(t) = t\left(\dfrac{g\tan\phi_{\text{nom}}}{v}\right) + \psi_0 \\ r(\psi(t) - \psi_0) = vt \end{cases} \tag{12}$$

Dividing the two equations leads to the radius as:

$$r = \frac{v^2(t)}{g\tan\phi_{\text{nom}}} \tag{13}$$

The distance d can be obtained by:

$$d = r\cot\frac{\theta}{2} = \frac{v^2}{g\tan\phi_{\text{nom}}}\cot\frac{\theta}{2} \tag{14}$$

(4) Breakout state (BS).

The aircraft breaks out of the corridor if the separation with its leading aircraft is less than the minimum separation, and also the lane switch requirement cannot be satisfied. BS is a terminal state in which the target aircraft follows a route to breakout to the side of a corridor as shown in Fig. 5. The

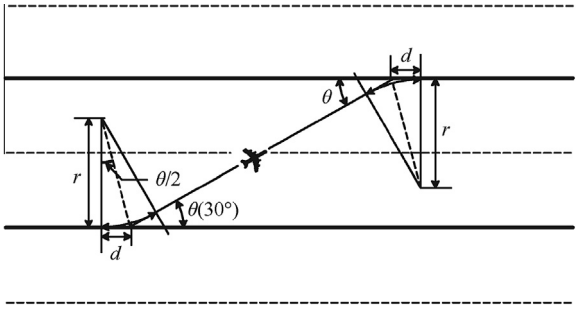

Fig. 4 Geometry of the fly-pass method.

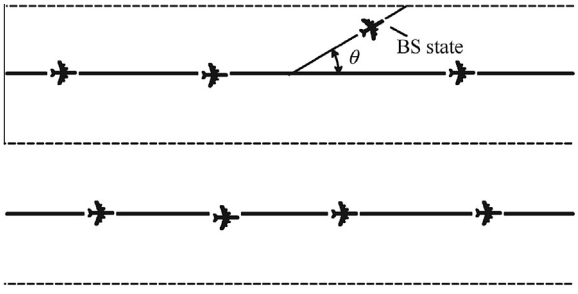

Fig. 5 Breakout state.

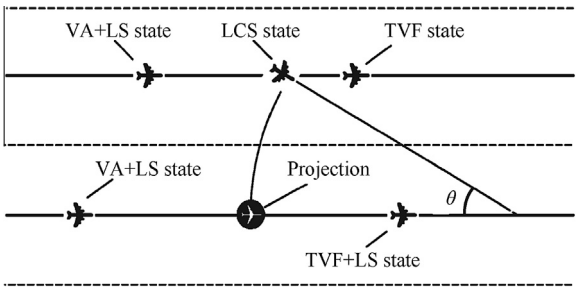

Fig. 6 Locking states.

breakout aircraft keeps its velocity and adjusts its 2D position until it is out of the corridor region. The trailing aircraft in the original corridor will be locked for one time step to avoid two consecutive aircraft changing to the BS or the LCS at the same time. This state can transfer from the VA state or the LCS (unidirectional transition).

(5) Locking state (LS).

LS is a combined state used for safety and efficiency consideration. This state always works with the VA and TVF states to prevent simultaneous lane changes or breakouts. For example, when the aircraft is in the LCS, the trailing aircraft in the original corridor will be in the LS (be locked) for one time step in order to avoid two consecutive aircraft changing to the LCS or the BS at the same time. Furthermore, the leading and trailing aircraft in the new corridor are locked until the corridor switch procedure is finished for safety. This is to prevent two aircraft from "crossing" in the middle while changing lanes. Fig. 6 illustrates a scenario of locking states.

2.2.3. Algorithm

In order to determine the throughput of the corridor, the aircraft performance model is established to capture the stochastic range of the problem. Table 3 defines some key variables in the main algorithm. Table 4 shows the pseudo code for the main algorithm. The core outline of the algorithm is briefly described. Specific details will be explained later.

In the loop, the algorithm checks the velocity differences and separations between the aircraft and their leading ones. If the velocity difference is equal to or greater than the velocity threshold, and also the current separation is less than the distance threshold, then the lane switch requirement will be checked. This represents a scenario where the trailing aircraft is traveling faster than the leading aircraft and the leading aircraft is not too far in front of the trailing aircraft, so the trailing aircraft wants to surpass the leading one. If the lane switch requirement is satisfied (the other lane is sufficiently clear, etc.), the trailing aircraft transfers to the lane switch state. If the trailing aircraft cannot switch lanes due to congestion, it transfers to the target velocity flying state, the velocity adjusting state, or the breakout state on the basis of different separations.

If the velocity difference is smaller than the velocity threshold, and also the current separation is larger than the distance threshold, the trailing aircraft changes to the target velocity flying state. Or else, the trailing aircraft will transfer to the velocity adjusting state when the current separation is between the distance threshold and the minimum separation. This represents a case where the trailing aircraft is traveling at a velocity that is either slower or only slightly faster than the leading aircraft. If the leading aircraft is sufficiently far in front, the trailing aircraft will simply be in the target velocity flying state; otherwise, it transfers to the velocity adjusting state to maintain separation with the leading one.

When the current separation is less than the minimum separation, the aircraft will be in the lane switch state if the lane switch requirement is satisfied, or else transfers to the breakout state.

3. Methodology for simulation

The en-route corridor model established above is neither completely discrete nor completely continuous. In order to analyze the risk-capacity tradeoff of the en-route corridor, a combined discrete–continuous simulation method is used to estimate the performance of the aircraft in the corridor.[14,15] The simulation was implemented in C++ language and displayed with Google Earth.[16] The simplified flowchart of the simulation is illustrated in Fig. 7.

3.1. Data process

Both practical data and Pseudo-random numbers are used in the simulation. The aircraft operation performance parameters used in this research come from the User Manual for the Base of Aircraft Data (BADA)[17] published by EUROCONTROL.

Table 3 Parameters for algorithm.

Variables	Description
Velocity difference	The velocity difference between the aircraft and its adjacent leading one
Velocity threshold	A threshold value of velocity used for triggering the transition of discrete states
Current separation	The longitudinal separation with its adjacent leading aircraft at current time
Minimum separation	The minimum separation requirement between adjacent aircraft for safety
Distance threshold	The threshold value of separation used for trigging transition of discrete states.
Lane switch requirement	Some clear requirement if the aircraft wants to switch its lane to another
Discrete states	Describe the movement of the aircraft in the corridor, including target velocity flying, velocity adjusting, lane change, breakout, and locking states

Table 4 Pseudo code for the main algorithm.

INPUT	Number of aircraft, simulation replication, corridor structure, time step, etc
INITIALZE	Aircraft types and initial attributes, minimum separation, target separation, etc
LOOP	**WHILE** not all aircraft passed the corridor DO
SIMULATE	Performance the movement simulation for all aircraft in the corridor
UPDATE	Aircraft discrete states as the following rules:
	If (velocity difference > velocity threshold)
	If (current separation > separation threshold)
	Target velocity flying state
	Else if (current separation > minimum separation)
	If (lane switch requirement is satisfied)
	Lane switch state
	Else
	Velocity adjusting state
	Else
	If (lane switch requirement is satisfied)
	Lane switch state
	Else
	Breakout state
	ELSE
	If (current separation > separation threshold)
	Target velocity flying state
	Else if (current separation > minimum separation)
	Velocity adjusting state
	Else
	If (lane switch requirement is satisfied)
	Lane switch state
	Else
	Breakout state
UPDATE	The queue length of aircraft in the corridor, and the simulation time
END OF LOOP	

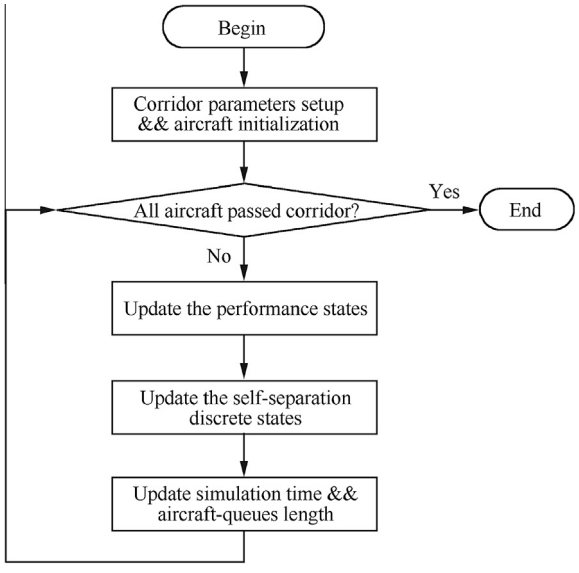

Fig. 7 Flowchart of simulation.

Eight typical aircraft types which are A320, A332, A345, A380, B737, B742, B743, and B764, are selected for simulations. The initial separations with the leading aircraft and the initial velocities of the target aircraft are generated randomly.

Table 5 Key input parameters.

Parameters	Description
Aircraft number	The number of aircraft generated for each lane to test the performance of the corridor
Replication times	The number of simulation iterations to analyze the risk-capacity tradeoff
Time step	The simulation time step for updating the states of the aircraft in the corridor
Initial separation	The initial separation with the leading one when the aircraft enters the corridor
Target separation	The separation aim that each aircraft attempts to keep with the leading one
Switch threshold	The minimum gap between the projection and the new leading/trailing aircraft for safe lane switching

3.2. Key variables

The computer simulation program includes 4 types of 68 different variables in total. Some of them have significant impacts on the performance of the corridor. Tables 5 and 6 define the key input and output parameters associated with the algorithm.[18]

3.2.1. Key input parameters

The key input parameters are the key static parameters that a user selects to run the simulation (Table 5). Note that

Table 6 Output metrics.

Parameters	Description
Capacity	The inverse of the average of the corridor passing time intervals
Breakout rate	The fraction of aircraft that breakout from the corridor
Switch rate	The fraction of aircraft that switch from one corridor to another
Conflict rate	The fraction of aircraft that either breakout or switch corridors

additional input parameters such as the target separation and the buffer separation are defined in Table 3 and not shown here.

3.2.2. Output metrics

These variables are the measures of system performance.[19,20] Currently, capacity, conflict rate, breakout rate, and lane switch rate are selected as the output metrics (Table 6). The collision risk is measured by conflict rate, breakout rate, and lane switch rate.

4. Simulation results

4.1. Case study

4.1.1. The aircraft flying by itself

Fig. 8 illustrates a sample scenario in which the aircraft flies by itself in the corridor. The x-axis corresponds to the time horizon when the aircraft is in the corridor. The y-axis corresponds to the velocities and accelerations during this time. This aircraft is a B737. It enters the corridor with a velocity of 456.25 knots and an acceleration of 0 knots/s. It maintains these values until it exits the corridor at simulation time 600 s.

4.1.2. The aircraft following another

Fig. 9 illustrates a typical scenario in which the aircraft follows another in the corridor. This aircraft is an A345. It enters the corridor at simulation time 2814 s with a velocity of 476.85 knots. Since the initial separation with the leading aircraft is large, it tries to reduce the gap by speeding up to 495.46 knots. Then it attempts to keep the target separation with the leading aircraft by slowing down. Once it becomes the first aircraft in the lane, it starts to fly towards its target velocity until exiting

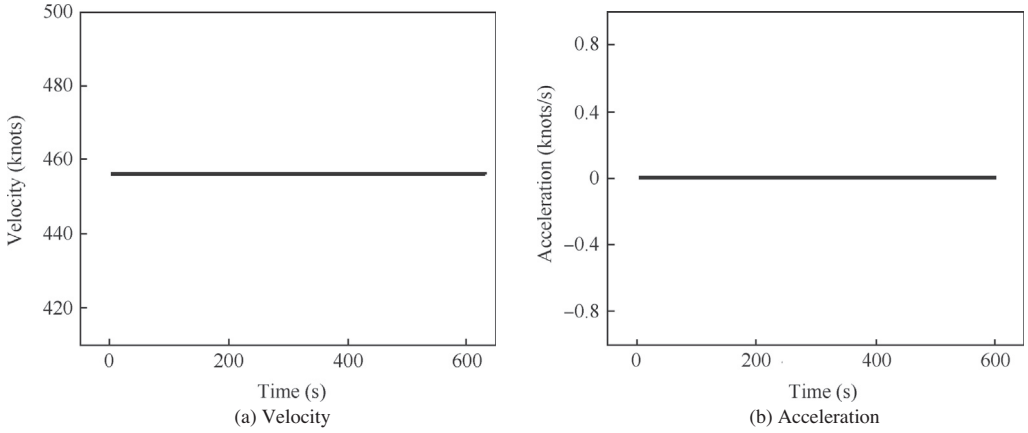

Fig. 8 B737 flying by itself.

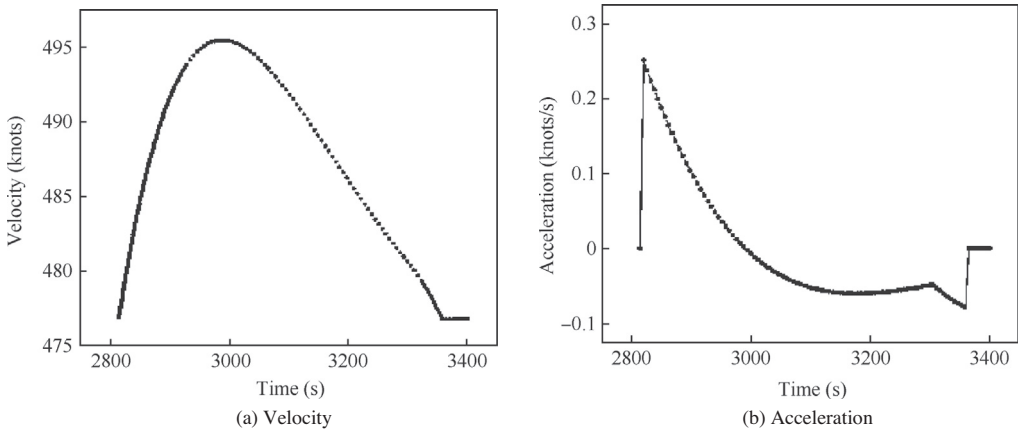

Fig. 9 A345 following another aircraft.

the corridor at simulation time 3402 s. The jump of the acceleration at simulation time 2800 s is caused by the start of self-separation with the leading aircraft in the corridor, and the jump at simulation time 3312 s is caused by the leading aircraft exiting from the corridor which makes the state of this aircraft change from VA to TVF. As the aircraft reaches its initial target velocity, the acceleration drops back to 0 at simulation time 3366 s finally.

4.1.3. The aircraft passing another

Fig. 10 illustrates a complex scenario in which the aircraft passing another by changing its lane. This aircraft is a B742. It enters the corridor at simulation time 936 s with a velocity of 513.4 knots. Because the initial velocity is so large, it tries to slow down to keep the minimum separation with the leading aircraft. At simulation time 984 s, it starts to switch lanes to pass the leading aircraft with a constant

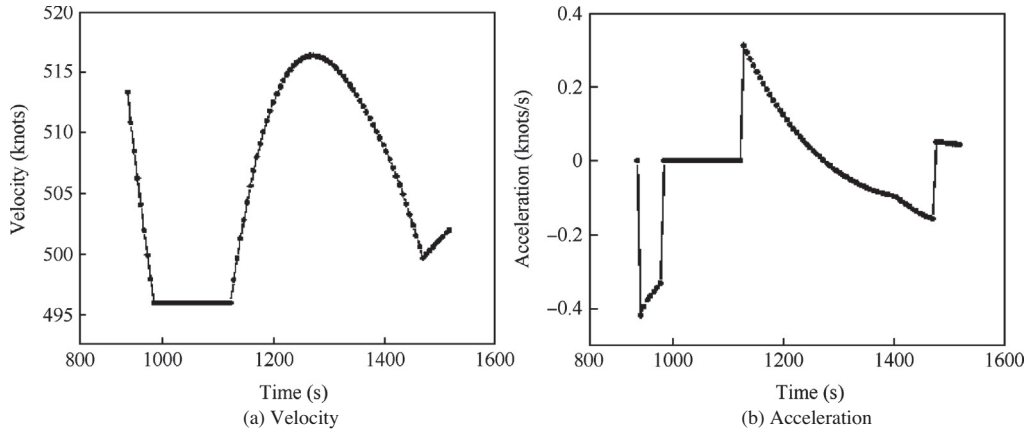

Fig. 10 B742 passing another aircraft.

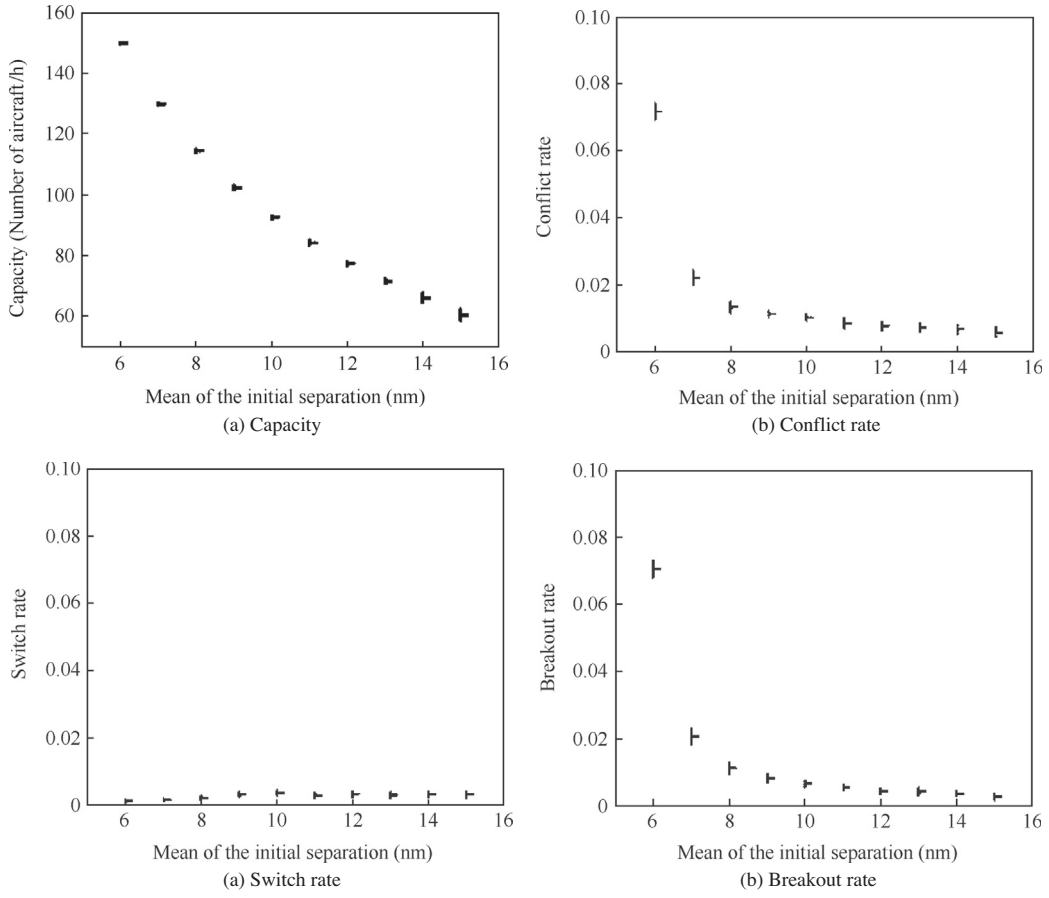

Fig. 11 Sensitivity analysis of initial separation.

velocity. After the lane changing, this aircraft adjusts its velocity and separation with the new leading aircraft until its exit of the corridor at simulation time 1518 s. The first jump of the acceleration is caused by changing the state from VA to LCS and the second jump is caused by changing back to VA. The reason of the third jump is caused by changing its state from VA to TVF as above.

4.2. Sensitivity analysis

4.2.1. Initial separation

The initial separations for the aircraft equal the sum of the minimum separation plus initial buffers which are independent and identically distributed (IID) exponential random variables. Fig. 11 illustrates the 95% confidence interval of the four output metrics by increasing the mean of initial buffers from 1 to 10 nm (this also indicates the mean of initial separations increasing from 6 to 15 nm) with 1 nm per step. The capacity has a monotone decrease from 150.4 to 62.3 number of aircraft/h while the switch rate has a very slight increase to 0.31%. The conflict and breakout rates drop rapidly by almost 71% when the initial separations increase to 7 nm, and after that they reduce slowly and decrease to 0.58% and 0.27%, respectively. Please note that the units of conflict rate, switch rate, and breakout rate are in fractional representation in all figures.

4.2.2. Target separation

The target separation for each aircraft equals the sum of the minimum separation plus a target buffer which is a constant. Fig. 12 illustrates the 95% confidence interval of the four output metrics by increasing the target buffer from 0.5 to 5 nm (this also indicates the target separation increasing from 5.5 to 10 nm) with 0.5 nm per step.

The capacity fluctuates slightly around 114.5 number of aircraft/h while the other three metrics fluctuate dramatically during the changing. Both the conflict and breakout rates decline sharply by almost 90% when the target separation increases to 7 nm. After that they begin to rise gradually and reach 23.5% and 17.2%, respectively. The switch rate has a similar trend and increases to 6.3% in the end. The changes of the difference between initial separation and target separation are the main reason of these trends. The corridor cannot accommodate so many aircraft within the corridor as the target separation increases, so the conflicts grow up again after reaching the bottom.

4.2.3. Distance threshold

The distance threshold for each aircraft is set as a constant. Fig. 13 illustrates the 95% confidence interval of the four output metrics by increasing the distance threshold from 7 to 16 nm with 1 nm per step. The capacity remains stable around 114 number of aircraft/h Conflict rate, switch rate, and break out rate fall moderately all the time and reach 1.45%, 0.325%, and 1.13%, respectively.

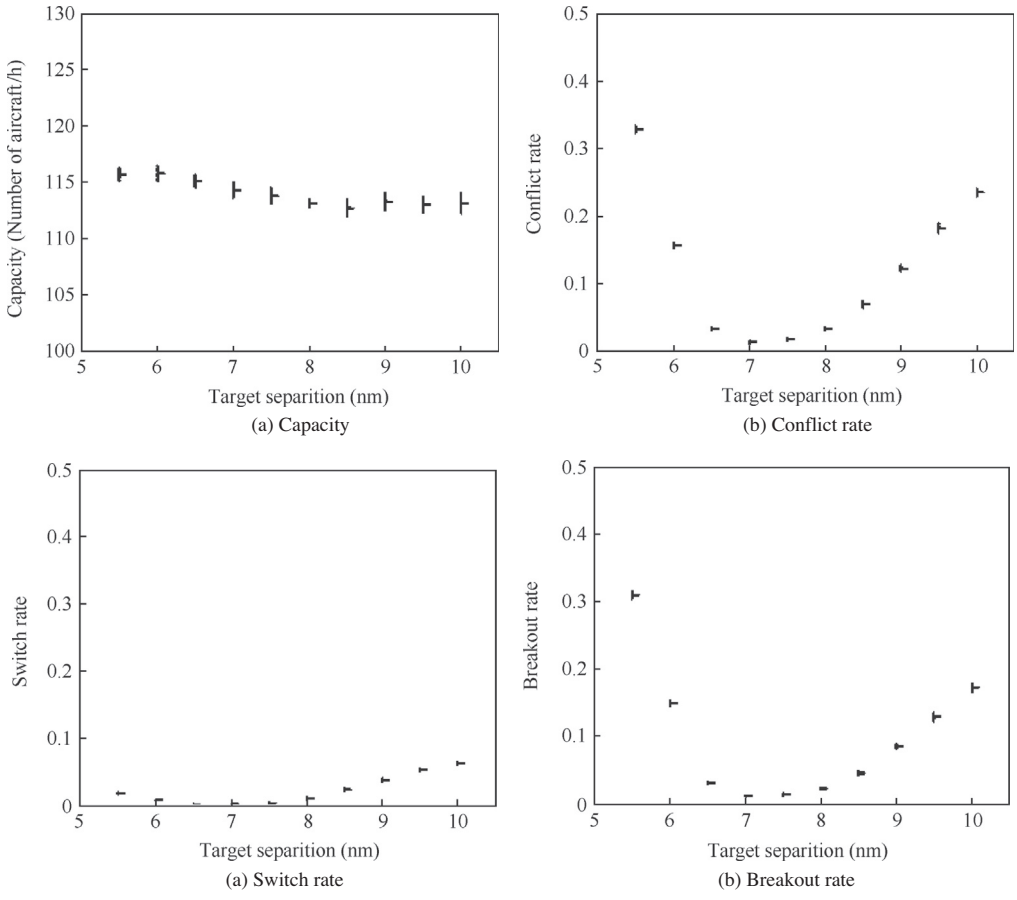

Fig. 12 Sensitivity analysis of target separation.

4.2.4. Switch threshold

The switch threshold for each aircraft is also set as a constant. Fig. 14 illustrates the 95% confidence interval of the four output metrics by increasing the switch threshold from 5.5 to 10 nm with 0.5 nm per step. The capacity remains stable at 114.5 number of aircraft/h. The conflict rate and switch rate have similar declining trends and reduce to 1.42% and 0.125%, respectively, while the breakout rate reaches a plateau at 1.3%.

5. Conclusions

The corridor concept is a revolutionary change of the current ATM system, which can reduce complexity and restructure the airspace to provide a higher system capacity. This paper conducted a reliability combined discrete–continuous simulation of aircraft flying in a self-separation corridor with two parallel routes, and filled up the research gap of new procedures initialization and safety analysis. According to the point mass model with the proportional derivative controller, each aircraft is simulated to adjust its acceleration, velocity, discrete state, etc. to fly through the corridor with safety, order, and high efficiency. Key insights from the model are:

(1) The initial separation between the aircraft has a significant effect on the capacity, conflict rate, and breakout rate of the corridor. As the mean of the initial separations increases, both the capacity and the collision decrease non-linearly. A good design of aircraft inter-arrival separation can lead to a high capacity with a low risk of conflict.
(2) The target minimum separation between pairs of aircraft is a very important variable. It's one of the key parameters in realizing aircraft self-separation in the corridor. Either too small or too large may lead to a high risk of conflict with no obvious improvement in the capacity.
(3) The distance threshold is an effective variable in reducing the conflict rate by limiting the chance of the aircraft flying at their preferred target velocities. A good distance threshold value may improve the rate and stability of the traffic flow in the corridor with a low risk of loss of separation.
(4) The switch threshold is a useful way in adjusting the switch rate of the corridor. However, no obviously effect has been found in improving the capacity and reducing the breakout rate.
(5) According to the experiments, when the mean of the initial separations is 8 nm, the target separation is 7 nm, the distance threshold is 12 nm, and the switch distance is 7 nm, the capacity and the collision risk will get the best tradeoff for the corridor structure in the paper.
(6) The main factor for the "system balance point" is relative to the discrete states transition rules which are established in Section 2.2.2 and the parameters setting of the proportional derivative controller. With a reason-

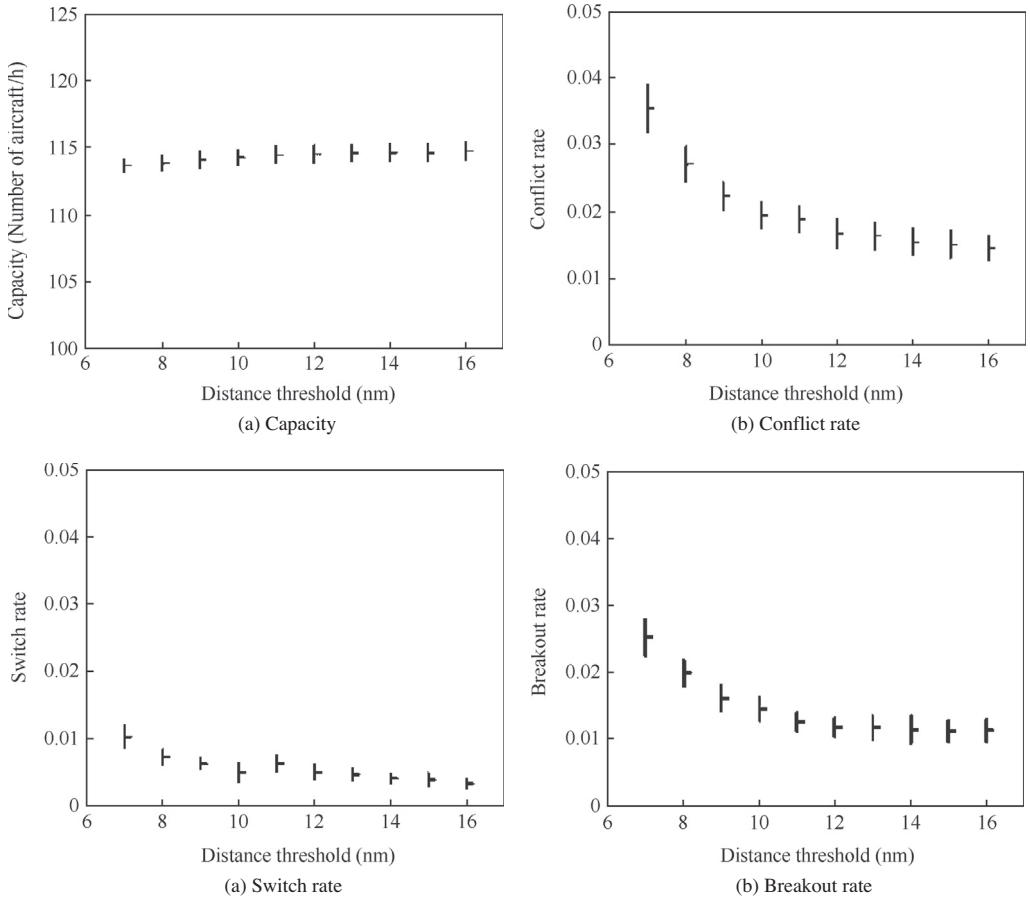

Fig. 13 Sensitivity analysis of distance threshold.

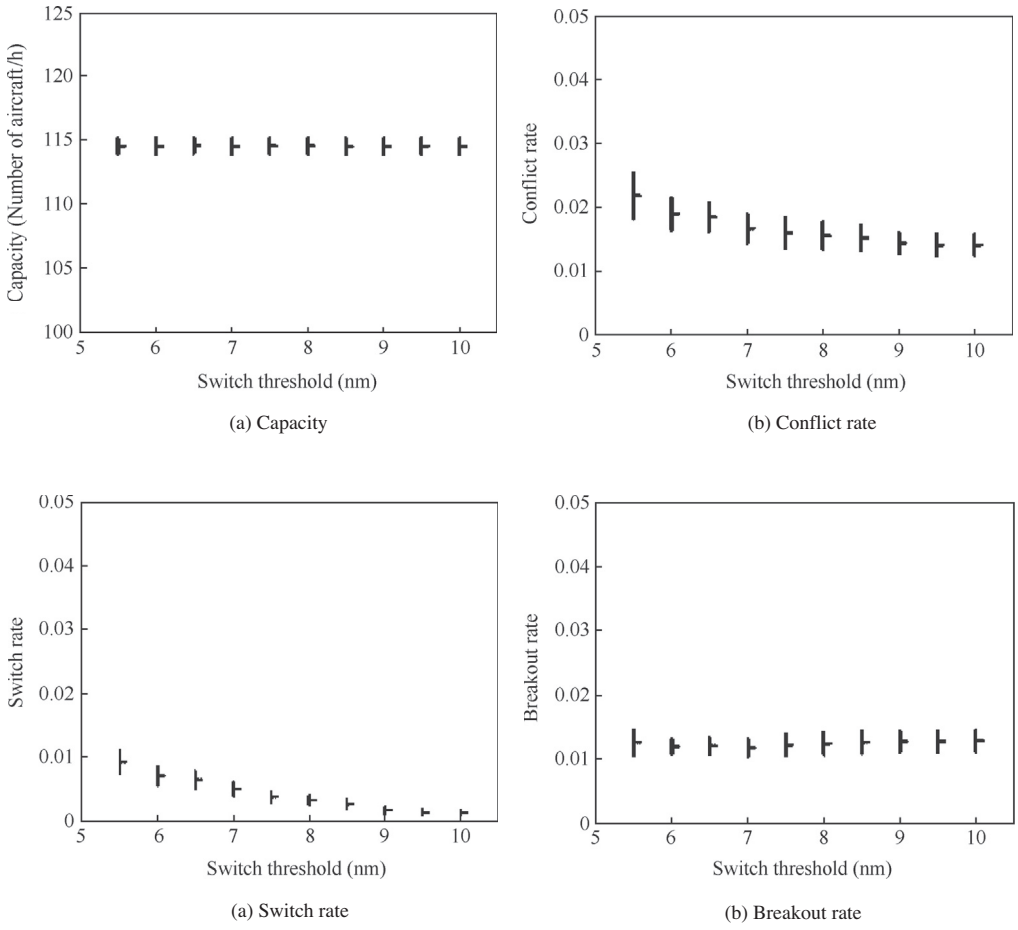

Fig. 14 Sensitivity analysis of switch threshold.

able target separation, distance threshold, and switch threshold, the collision risk may decrease without serious impact on the capacity of the corridor.

(7) Some side routes or transition regions should be carefully designed for avoiding small probability event risk in the corridor.

(8) The corridor structure presented in this paper is relatively basic. Future work includes extending the corridor structure to two or more levels and introducing vertical movements of aircraft with time lag and random error. The interactions between different parameters are another work to be done.

Acknowledgements

The authors thank Dr. George Donohue, Dr. Lance Sherry, and Dr. Chun-Hung Chen for suggestions and helps. The work was supported by the National Natural Science Foundation of China (No. 61104159), National Science and Technology Support Project (2011BAH24B08) and the National High-tech Research and Development Program of China (No. 2011BAH24B08).

References

1. Joint Planning and Development Office. *Concept of operations for the next generation air transportation system*. Washington, DC; 2010.
2. John A, Patricia C, Hong K, Noreen S, Omar S, George LD, et al. Dynamic airspace super sectors (DASS) as high-density highways in the sky for a new US air traffic management system. In: *Proceedings of 2003 systems and information engineering design symposium, April 24–25*; 2003. p. 57–66.
3. Yousefi A, Donohue G, Sherry L. High-volume tube-shape sectors (HTS): a network of high capacity ribbons connecting congested city pairs. In: *Proceedings of 23rd digital avionics systems conference, October 24–28*; 2004. p. 3.C.1(1)–3.C.1(7).
4. Sridhar B, Grabbe S, Sheth K, Bilimoria K. Initial study of tube networks for flexible airspace utilization. In: *Proceedings of 2006 AIAA guidance navigation and control conference, August 21–24*; 2006; AIAA-2006-6768.
5. Hoffman R, Prete J. Principles of airspace tube design for dynamic airspace configuration. In: *Proceedings of 8th AIAA-ATIO conference, September 14–19*; 2008. AIAA-2008-8939.
6. Xue M, Kopardekar PH. High-capacity tube network design using the Hough transform. *J Guid Control Dyn* 2009;**32**(3):788–95.
7. Xue M, Zelinski S. Complexity analysis of traffic in corridors-in-the-sky. In: *Proceedings of 10th aviation technology, integration, and operations conference, September 13–15*; 2010. AIAA-2010-9112.
8. Yousefi A, Zadeh AN, Tafazzoli A. Dynamic allocation and benefit assessment of NextGen flow corridors. *Transp Res Part C* 2013;**33**(SI):297–310.
9. Yousefi A, Lard J, Timmerman J. Nextgen flow corridors initial design, procedures, and display functionalities. In: *Proceedings of 29th IEEE/AIAA digital avionics systems conference (DASC), October 3–7*; 2010. p. 4.D.1(1)–4.D.1(19).

10. Glover W, Lygeros J. A multi-aircraft model for conflict detection and resolution algorithm evaluation. Deliverable D1.3. European Commission; 2004 February Contract No.: IST-2001-32460 of European Commission.
11. William JP. *System dynamics*. 2nd ed. McGraw-Hill Higher Education; 2009.
12. Erzberger H. Automated conflict resolution for air traffic control. In: *Proceedings of 25th international congress of the aeronautical sciences, September 3–8*; 2006. p. 1–27.
13. McNally D, Thipphavong D. Automated separation assurance in the presence of uncertainty. In: *Proceedings of 26th international congress of the aeronautical sciences, September 15–19*; 2008; ICAS-2008-8.8.
14. Law AM, Kelton WD. *Simulation modeling & analysis*. 4th ed. McGraw-Hill Higher Education; 2007.
15. Chen CH, Lee LH. *Stochastic simulation optimization: an optimal computing budget allocation*. New Jersey: World Scientific Publishing Co. Inc.; 2010.
16. Chadil N, Russameesawang A, Keeratiwintakorn P. Real-time tracking management system using GPS, GPRS and Google earth. In: *Proceedings of 5th international conference on electrical engineering/electronics, computer, telecommunications and information technology, May 14–17*; 2008. p. 393–6.
17. European Organization for the Safety of Air Navigation, EUROCONTROL Experimental Centre. User manual for the base of aircraft data (BADA). Revision 3.6, 2004 July. Report No.: EEC Note No. 10/04.
18. Ye BJ, Hu MH, John S. Risk-capacity tradeoff analysis of an en-route corridor model. In: *Proceedings of 5th international conference on research in air transportation, May 22–25*. Berkeley, US; 2012.
19. Sherali HD, Hill JM, McCrea MV, Trani AA. Integrating slot exchange, safety, capacity, and equity mechanisms within an airspace flow program. *Transp Sci* 2011;**45**(2):271–84.
20. Castelli L, Pesenti R, Ranieri A. The design of a market mechanism to allocate air traffic flow management slots. *Transp Res Part C: Emerg Technol* 2011;**19**(5):931–43.

Ye Bojia is a Ph.D. student in the College of Civil Aviation at Nanjing University of Aeronautics and Astronautics. He visited the Center for Air Transportation Systems Research at George Mason University from 2010 to 2012. His area of research includes air traffic flow management, multi-agent system modeling and simulation, etc.

Hu Minghua is a professor and Ph.D. advisor in the College of Civil Aviation at Nanjing University of Aeronautics and Astronautics, and the director of the National Key Laboratory of Air Traffic Flow Management. His current research interests are air traffic flow theory, air traffic flow management, ATFM assessment theory and methodology.

John Friedrich Shortle is an associate professor in the Volgenau School of Engineering at George Mason University, U.S. He received his M.S. and Ph.D. degrees from University of California, Berkeley in 1993 and 1996, respectively. His current research interests are queuing theory, simulation, telecommunications, air transportation, etc.